Energies **2013**, *6*, 6170-6187; doi:10.3390/en6126170

OPEN ACCESS

energies

ISSN 1996-1073

www.mdpi.com/journal/energies

Article

Co-Combustion of Animal Waste in a Commercial Waste-to-Energy BFB Boiler

Farzad Moradian [1,*], Anita Pettersson [1], Solvie Herstad Svärd [2] and Tobias Richards [1]

[1] School of Engineering, University of Borås, Allégatan 1, 50190 Borås, Sweden; E-Mails: anita.pettersson@hb.se (A.P.); tobias.richards@hb.se (T.R.)

[2] Scandinavian Energy Project AB, Rullagergatan 4, 41526 Göteborg, Sweden; E-Mail: solvie.herstad.svard@wspgroup.se

* Author to whom correspondence should be addressed; E-Mail: farzad.moradian@hb.se; Tel.: +46-33-435-4855; Fax: +46-33-435-4008.

Received: 26 September 2013; in revised form: 16 November 2013 / Accepted: 21 November 2013 / Published: 27 November 2013

Abstract: Co-combustion of animal waste, in waste-to-energy boilers, is considered a method to produce both heat and power and to dispose of possibly infected animal wastes. This research conducted full-scale combustion tests to identify the impact of changed fuel composition on a fluidized-bed boiler. The impact was characterized by analyzing the deposit formation rate, deposit composition, ash composition, and emissions. Two combustion tests, denoted the reference case and animal waste case, were performed based on different fuel mixes. In the reference case, a normal solid waste fuel mix was combusted in the boiler, containing sorted industry and household waste. In the animal waste case, 20 wt% animal waste was added to the reference fuel mix. The collected samples, comprising sampling probe deposits, fuel mixes, bed ash, return sand, boiler ash, cyclone ash and filter ash, were analyzed using chemical fractionation, SEM-EDX and XRD. The results indicate decreased deposit formation due to animal waste co-combustion. SEM-EDX and chemical fractionation identified higher concentrations of P, Ca, S, and Cl in the bed materials in the animal waste case. Moreover, the risk of bed agglomeration was lower in the animal waste case and also a decreased rate of NO_x and SO_2 emissions were observed.

Keywords: bubbling fluidized bed (BFB) boiler; animal waste; MSW; deposit; ash

1. Introduction

Increasing demand for sustainable heat and power production, as well as problems landfilling wastes, has prompted heat and power plants to replace fossil fuels with alternatives such as combustible municipal solid wastes (MSW) or refuse-derived fuels (RDF) [1,2]. Combustion of MSW and RDF, however, can lead to serious fouling and corrosion problems, due to their physical and chemical properties. The major difficulties with thermally processing waste fuels are attributed to their heterogeneity, high concentrations of alkali and chlorine, and high content of inorganic incombustible materials [3]. Fluidized-bed boilers, with their inherent fuel flexibility, have been developed to resolve problems concerning fuel heterogeneity and high ash content [4]. High concentrations of alkali and chlorine compounds could cause severe corrosion of steel surfaces, particularly at temperatures above 450 °C. Potassium, sodium, and chlorine are known to be the main causes of severe high-temperature corrosion [5]. In addition, interaction between alkali species and silica sand leads to the formation of low-temperature eutectics, which could cause the agglomeration/defluidization of fluidized-bed boilers [6]. Formation of bed and fly ashes, which may contain large amounts of potentially toxic metal compounds, is also a problem when waste fuels are combusted. These ashes, which could harm the environment, are classified as hazardous materials and need special treatment and storage when landfilled [7].

Regardless of these problems, the combustion of waste fuels is still an interesting option, considering their often high energy content, their abundance, and the economic aspects of combusting them. Improved boiler operation has been investigated by either modifying the boiler function or changing the fuel mix. For example, a previous full-scale project, the Reduced-Bed Temperature (RBT) project [8], reduced the bed temperature by recirculating flue gas and spraying water on the fuel to modify the boiler function. The outcome was positive in terms of deposit formation rate, fly ash flow rate, reduced risk of bed agglomeration and some capture of chlorine in the bed [8]. Co-combustion and additive use have also proved useful in alleviating the addressed problems. Co-combustion of secondary waste fuels, such as sewage sludge and animal waste, has previously shown benefits in some projects [9–11]. Animal waste, a new fuel type, has proved beneficial when co-fired with wood chips, sorted MSW, and peat in commercial boilers [11].

The present research investigated co-combustion of animal waste with a mix of sorted industrial and sorted household waste, in a full-scale bubbling fluidized bed (BFB) boiler. The paper investigates the impact of the new fuel composition on the boiler operation. Especially the effects on operational issues, such as deposition growth rate in the heat transfer area, bed agglomeration and flue gas emissions, were followed. The distribution of major ash forming elements such as Ca, S, Cl, Na, K and P in the bed and fly ashes were examined. It was particularly significant to find out how the high concentrations of calcium phosphate compounds in the animal waste and its high moisture content [11] affected the ash transformation behavior in the bed area. Analysis of the formed deposit on the deposit rings was also performed to determine the amount of corrosive elements such as Cl and alkalis. A series of complementary lab-scale tests were also conducted to determine the effect of animal waste co-combustion on bed agglomeration temperature. The emissions of NO_x in the flue gas were measured, to identify whether high nitrogen content of animal waste [11] may change NO_x emissions in positive or negative way.

2. Experimental

2.1. The Fuel

Since the 2000s, the incineration of animal wastes classed at high risk of being infectious, such as animal carcasses and slaughterhouse waste products, has been regulated by the EU Commission, due to the bovine spongiform encephalopathy (BSE) crisis in the European beef industry [11,12]. Apart from sanitary considerations, the acceptable heating value of animal waste, approximately 7–8 $MJ \cdot kg^{-1}$, make it an interesting co-fuel for waste-to-energy boilers [11]. The animal waste is crushed and grinded into a slurry (Figure 1) in a separate plant, and transported to a receiving tank at the combustion plant. From the receiving tank, the slurry is pumped into the boiler through a closed pipe system [11]. The slurry which was injected to the boiler consists of two fractions; hard tissue (bone) and soft tissue (fat and protein) which have high concentrations of calcium phosphate compounds.

Figure 1. Crushed and ground animal waste prepared for combustion.

Two tests were performed with fuels of different compositions, referred to as the reference (Ref) and the animal waste (AW) cases. The fuel used in the Ref case was the ordinary waste fuel mix usually used in this boiler, consisting of 70 wt% sorted and pretreated industrial waste (RDF) and 30 wt% sorted and pretreated household waste (MSW). The waste fuel mix (MSW and RDF) consists mainly of paper, plastic, and wood and has a moisture content of approximately 35%, which is below what the boiler was designed to handle. In the AW case, 20–30 wt% of AW, representing approximately 20% of the total energy content of the fuel mix, was added as secondary fuel to the ordinary waste fuel mix. All fuels were grinded to a particle size <100 mm, which is the designed fuel size for this boiler.

2.2. The Boiler

Full-scale tests were conducted in a 20 MWth BFB boiler designed for waste combustion (Figure 2) owned by Borås Energy and Environment AB. The plant launched the co-combustion of AW with the ordinary waste fuel mix in the autumn of 2010. The tests were carried out in boiler No. 1 of the two twin boilers, which is equipped with measurement openings in the walls and equipment for fuel and ash sampling. Boiler No. 1 operates parallel to boiler No. 2, both of which use the same fuel feeding and ash transportation system. These boilers produce superheated steam of 405 °C and 49 bar, used for power and heat production. The boilers are designed for a bed temperature of 870 °C, but due to decreased bed agglomeration and lower deposition growth rate in the RBT project [8], the goal is a bed temperature of 750 °C.

Figure 2. Ash sampling and measurement positions: (1) Bed ash; (2) Boiler ash; (3) Cyclone ash; and (4) Deposit probes upstream of the superheaters.

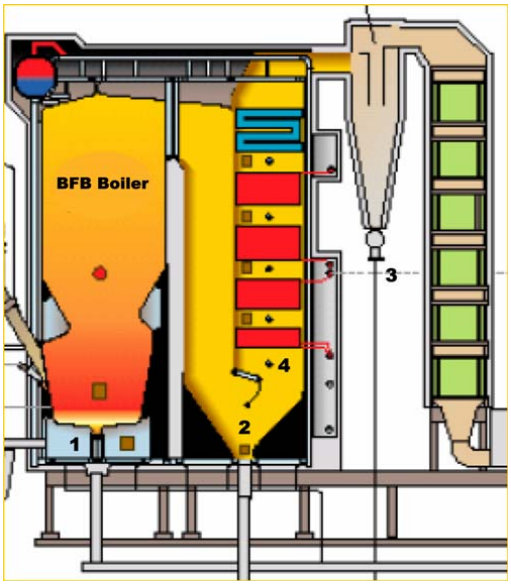

2.3. The Tests

The full-scale co-combustion tests were carried out with typical operation conditions for a BF-boiler. Also bed sand, fuel size, moisture in with fuel and fluidization of the boiler corresponded to normal conditions. The experimental procedure entails sampling the return sand, bed and fly ashes, and deposits collected on a deposit probe, in addition to analyzing the flue gases emitted for two fuel compositions: the Ref and AW cases. Before each test, the boilers were operated with the desired fuel mixture for at least three days to eliminate any memory effects of the previous fuel. In deposit sampling, a deposit probe, simulating the super-heater tubes, was inserted upstream of the superheaters (No. 4 in Figure 2) where the flue gas has temperature of approximately 630 °C. The deposition analysis was repeated twice, once in the morning and once in the afternoon. The surface of the deposit probe was maintained at a temperature of 435 °C in all tests, representing a steam temperature of 405 °C, corresponding to normal boiler performance. The probe was equipped with two high-alloyed steel rings, one for elemental analysis and one for SEM-EDX analysis of the collected material. The exposure time for each sampling was three hours.

Bed materials, return sand, and fly ashes were sampled continuously during the combustion tests, to examine the effects of the two fuel compositions on bed agglomeration and ash chemistry. The bed material consists of both coarse and fine fractions. The coarse fraction of the bed material is discharged as bed ash (No. 1 in Figure 2), while the fine fraction, comprising mostly bed sand, is recycled to the boiler after sieving (return sand). In addition, the level of bed material is maintained by continuously injecting fresh sand into the bed area. The fly ashes, *i.e.*, boiler ash, cyclone ash, and filter ash, were collected from the empty pass, cyclone, and textile filter, respectively. For each ash fraction and each fuel blend, sampling was repeated four times, at two hour intervals for each sampling. To obtain a mean value, a mixture of the four samples of each fraction was sent to the laboratory [13]. The emission rates of H_2O, CO_2, SO_2, CO, NO_x, HCl, NH_3, and N_2O in the flue gas were continuously analyzed using Fourier Transform Infra-Red (FTIR) spectrometry (ABB Bomem Inc., Quebec, Canada).

2.4. The Analysis

2.4.1. SEM-EDX

A scanning electron microscope (FEI Quanta 200 ESEM FEG) (Oxford instruments Inc., Abingdon, UK) equipped with Oxford Inca Energy Dispersive X-ray (EDX) (Oxford instruments Inc., Abingdon, UK) was used for elemental analysis of ash particles. In particular, the topography was examined using SEM, while the distribution of key elements, including both qualitative and quantitative analysis, was performed using EDX. As surface preparation, ashes were mounted in epoxy and polished before the cross-sectional SEM-EDX analysis.

2.4.2. Chemical Fractionation

Chemical fractionation, a progressive leaching method using various solvents, has proven useful to estimate whether compounds in the fuel are reactive or inert during combustion [14]. With this method, an indication of the ash chemistry could be obtained; it could also be applied to determine the compound composition of ashes as a complementary method to SEM-EDX analysis [15]. The method was used for analyzing boiler and cyclone ashes in addition to the coating layer on return sand particles.

In the first step of chemical fractionation, deionized water is used to extract water-soluble compounds such as alkali sulfates, carbonates and chlorides. Recent studies indicate that some phosphates can also be extracted [16]. In the second step, carbonates, as well as sulfates, which are not easily dissolved by water, are leached out using ammonium acetate, NH_4Ac [15]. The fractions that are insoluble in water or ammonium acetate are considered less reactive during combustion. In the last step of the fractionation, other phosphates, carbonates and sulfates are extracted using 1.0 M HCl at 70 °C. The remaining solid residue, an insoluble fraction, consists of silicates and other compounds such as oxides, sulfides and minerals [15,16].

An inductive coupled plasma with atomic emission spectroscopy (ICP–AES) detector and an inductive coupled plasma with mass spectrometry (ICP–MS) detector were employed to analyze Ca, Al, Fe, K, Mg, Na, P, Si, S, Cl, and Ti in the leachates and solid samples. All solid samples were entirely dissolved according to Swedish standards SS028311 and SS028150-2 [17] before analysis.

2.4.3. Bed Agglomeration Test

To compare the bed agglomeration behavior, a series of complementary lab-scale tests was conducted. The return sands collected from the full-scale tests were put in a lab-scale fluidized-bed combustor to assess the consequences of AW co-combustion on bed agglomeration. The combustor was initially stabilized at 750 °C and fluidizing gas (85% N_2 and 15% CO_2) was uniformly introduced through the bed, 68 mm in diameter, at a rate of 50 L min^{-1}. The temperature was gradually increased from 750 °C to 1100 °C at a rate of 3.5 °C min^{-1}, while the pressure was continuously monitored across the bed. The first pressure drop gives the initial point when sand particles start to sinter together, which is called the partial agglomeration temperature. The total agglomeration temperature occurs when the slope of the pressure drop starts to increase; *i.e.*, the decrease is no longer sharp. The method

is estimated to be accurate to within ±10 °C. This measurement, however, is comparative between the cases and cannot be directly used in a full-scale boiler [18].

2.4.4. XRD

X-ray diffraction (XRD) was used to determine the chemical composition of the crystalline compounds found in the ash fractions. The XRD data presented were obtained from a Siemens D5000 X-ray powder diffractometer (Siemens AG Inc., Munich, Germany) using the characteristic Cu radiation, and a scintillation detector. The JCPDS database, version 2010 (ICDD, Pennsylvania, USA), was used as a standard when identifying the crystalline compounds present in the ashes.

3. Results and Discussion

3.1. Fuel Analysis

The results of the fuel analyses are presented in Table 1. The ash content of the AW is almost half that of the ordinary MSW, making the ash content slightly lower in the resulting fuel mix. The calorific value of the fuel mix, however, decreased from 10.9 MJ kg^{-1} to 9.4 MJ kg^{-1} with the addition of wet AW.

Table 1. Fuel analysis.

Fuel		MSW (Ref)	AW	AW + MSW (AW)	Method
Moist, raw, wt-%		37.5	60.9	46.4	CEN/TS 14774-2
Ash, dry, wt-%		20.3	13.7	18.4	CEN/TS 14775
Dry sample, wt-%	C	46.9	54.3	47.1	CEN/TS 15104
	H	6.20	7.90	6.30	CEN/TS 15104
	N	1.20	6.30	1.80	CEN/TS 15104
	O	24.3	17.3	25.3	Calculated
	S	0.46	0.30	0.40	CEN/TS 15289
	Cl	0.70	0.40	0.70	CEN/TS 15289
LHV, raw, MJ kg^{-1}		10.9	8.30	9.40	CEN/TS 14918
HHV, raw, MJ kg^{-1}		18.8	25.0	19.7	CEN/TS 14918
Ash analysis, mg kg^{-1} ash	K	3,898	2,050	2,926	ASTM D 3682
	Na	6,557	4,550	6,009	ASTM D 3682
	Ca	27,405	45,100	33,876	ASTM D 3682
	Al	11,611	<100	9,447	ASTM D 3682
	Mg	2,740	1000	3,001	ASTM D 3682
	Ti	1,603	<100	2,437	ASTM D 3682
	Mn	223	<100	183	ASTM D 3682
	P	954	21,900	4,252	ASTM D 3682
	Fe	4,993	400	6,035	ASTM D 3682
	Zn	893	2,500	1,043	ASTM D 3683
	Pb	1,482	<10	350	ASTM D 3683

Table 1 also shows that the concentration of N is much higher in AW compared to the ordinary waste mix. The elemental analysis presented in Figure 3 indicates significantly more P, and Ca and less S, Cl, Na, and K in AW than in the ordinary waste mix. The resulting fuel mix of ordinary waste fuel and AW contains a four times higher phosphorus concentration than does the ordinary waste mix. Note that, due to the characteristics of waste fuels, the composition of this fuel changes over time and was not exactly the same for all tests.

Figure 3. Composition of fuels and fuel mix.

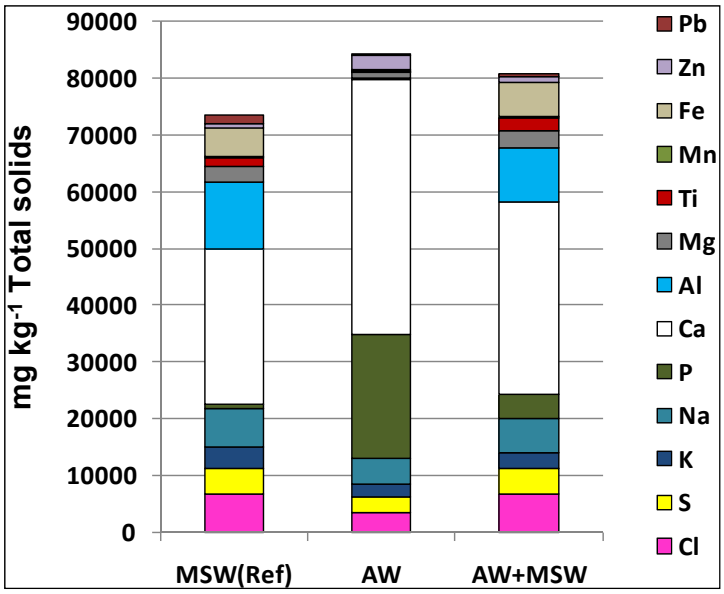

3.2. Deposit Formation

The deposits formed on the surface of the rings during the various combustion tests are illustrated in Figure 4. In addition, Figure 5 shows the deposition growth rate and corresponding elemental analysis for the sampled deposit for each combustion test. The results indicate a reduction in the rate of deposit formation during AW co-combustion by three times.

Figure 4. Deposit formed on the rings.

Figure 5. Deposition growth rate and elemental analysis for the Ref and AW cases.

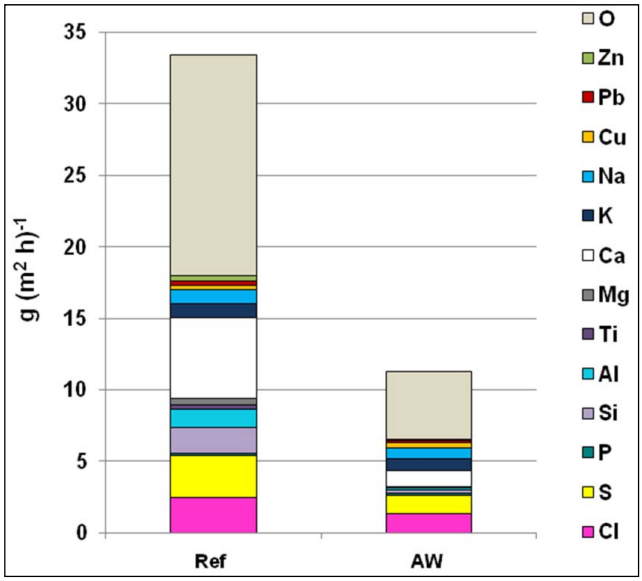

Regarding the elemental distribution on the rings, the Cl concentration (11 wt%) in the deposit was higher in the AW case than the 7 wt% in the Ref case. However, the total amount was lower in the AW case than in the Ref case. The total alkali concentration rose from 6 wt% in the Ref case to approximately 14 wt% for the AW case. Moreover, the increased amount of Ca and P in the fuel (Figure 3) is not reflected in the deposit composition. The Ca concentration was 30 wt% lower and P was at the same level in the deposits formed during the AW case versus the Ref case. In addition Si and Al were found in lower concentrations in the deposits in the AW case. The concentration of S, however, increased by 33.5 wt% in the AW case.

Even though the deposit rings indicate a reduction in the amount of deposit formed in the AW case, a higher risk of corrosion might be expected due to the increased concentration of alkali and chlorine. However, visual inspection of the boiler tubes after almost one year of co-combustion with AW, did not reveal any increased corrosion.

3.3. SEM-EDX Analysis on Ashes

SEM-EDX was employed to perform elemental analysis of the coating layers formed during combustion on the particles of sampled return sand and boiler ash. The analyses presented here focus mainly on the return sand, though the coating on the boiler ash was similar in nature. Two types of sand particles are present in the boiler, consisting of silicon oxides or feldspar. Therefore, it was important to determine whether their original composition could have affected the compounds bonding to their surface during combustion. The results, however, showed no indications of differences between the particles and, in contrast to previous findings, no signs could be found of alkali silicate melt on the inner surface of the silica sand particles [6,19,20].

Figures 6a,b shows cross-sectional SEM-EDX spot analyses of the entire coating from its outer layer to the surface of the sand particles, for two return sands from the Ref and AW cases. The corresponding elemental distributions of Cl, S, Ca, Na, P, Al and Si are presented in Figure 6c,d. Comparison of the two cases indicates that the concentrations of Ca, S, Cl and P are higher in the

coating layer on return sand from the AW case. Si and Al, however, are found to be slightly lower in this case. The higher concentrations of Na, Si, and Al at point No. 8 in both cases reflect the original compositions of the feldspars in the sand particles.

Figure 6. Cross-sectional SEM-EDX spot analysis of the coated return sands: (**a**) and (**c**) for the Ref case; (**b**) and (**d**) for the AW case.

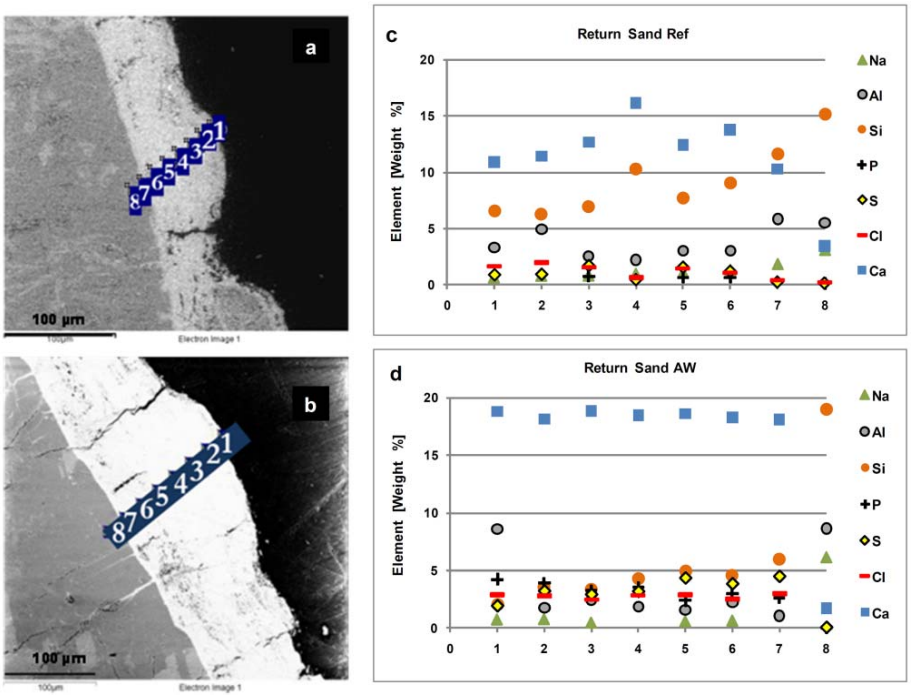

To achieve an average coating composition, three of the analyzed sand particles were picked from each combustion test. The results presented in Figure 7 confirm the higher concentrations of Ca, Cl, P, and S (which increased by 4.3, 1.3, 2.4 and 1.8 wt%, respectively) in the coating of the return sand particles in the AW case compared to the Ref case. The same coating composition was also found on the bed ash material and on the boiler ash particles. Higher capture of Ca, S, Cl and P compounds in the bed area could be connected to the lower rate of deposit formation in the super heater area. The results for alkali (Na, K), however, did not indicate any notable differences between the two cases, suggesting that the changed boiler conditions did not significantly affect the alkali capture in the bed.

Figure 7. Average element concentrations in the coating surrounding the sand particles.

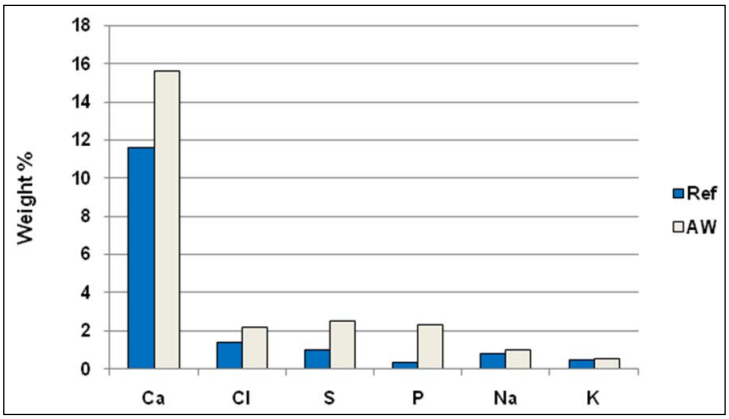

3.4. Chemical Fractionation Results for Return Sand and Cyclone Ash

The chemical fractionation results for the particles more or less support the results obtained using SEM-EDX. As Figure 8 shows, higher concentrations of Ca, S, and P could be observed in the coating of the sand particles in the AW case, while the difference between the concentrations of Na and K are small. Note also that the largest part of the alkali found in the non-soluble fraction originates from the feldspar particles in the sand.

Figure 8. Results of chemical fractionation analysis of return sands with coatings: (**a**) Ref; (**b**) AW.

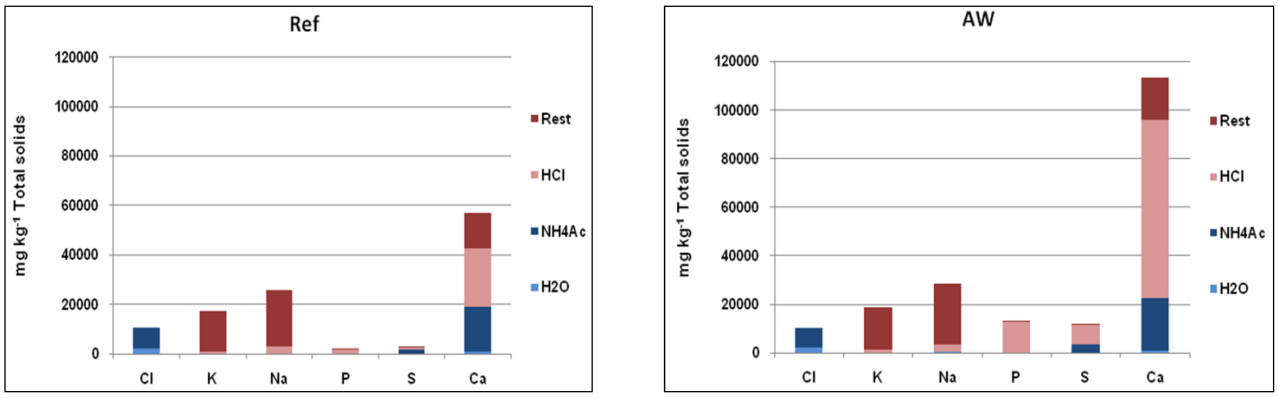

(**a**) (**b**)

Comparing the two cases, the major differences in the concentrations of Ca, S, and P are found in the acid-soluble fractions. The water-and acetate-soluble fractions, in addition to the insoluble portions of Ca, P, and S are almost the same in both cases. All of the extra Ca, S, and P is found in acid-soluble forms in the AW case. This was partly explained by the fact that AW is rich in crushed bone containing $Ca_{10}(PO_4)_6(OH)_2$ and β-$Ca_3(PO_4)_2$ [11,12,21], which is soluble in acid. But in addition, parts of the P introduced with the AW fuel derive from proteins in the soft tissue of the animals and are reactive during combustion [22]. This reactive part of P dominates over Si in the competition for Ca^{+2} to form calcium-phosphate, which is a stable compound [23].

The results of chemical fractionation of cyclone ash are presented in Figure 9. In addition, the concentration of acid-soluble Ca and P apparently increased in the AW case. The solubility of S changed drastically when adding AW. In the Ref case, the largest part of S occurred as acetate-soluble compounds, but in the AW case most S was found as acid-soluble compounds. The results do not indicate in which form this S is found in the ash. For the boiler ash, the results are almost similar to the cyclone ash.

Figure 9. Results of chemical fractionation analysis of cyclone ash.

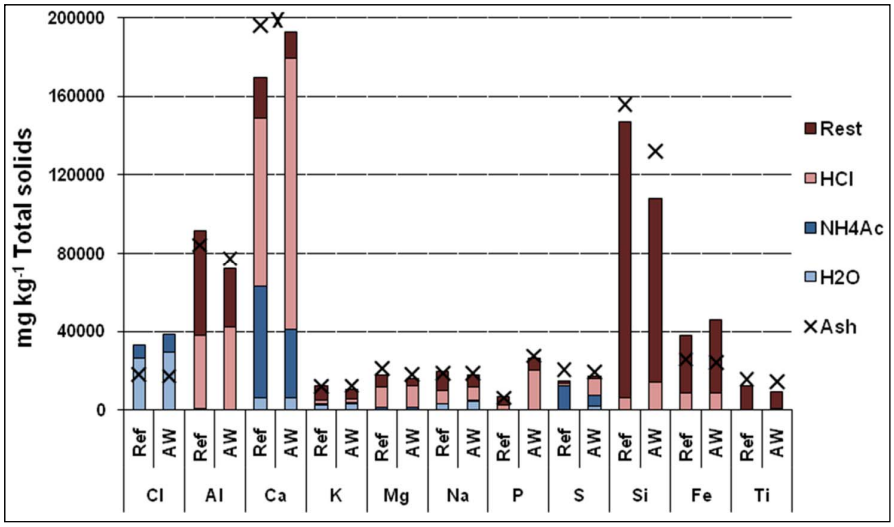

3.5. XRD

The XRD results for boiler ash, cyclone ash, filter ash and fresh sand are presented in Table 2. The differences between the three cases are very small, probably due to the original composition of the fresh sand. The ordinary composition of Swedish sands, which contain feldspars, make it difficult to distinguish, analytically, between the sands and ashes. Quartz (SiO_2), albite ($NaAlSi_3O_8$), microklin ($KAlSi_3O_8$) and klinoklor ($(Mg,Al)_6(Si,Al)_4O_{10}(OH)_8$) are compounds found in the fresh sand. Several of these compounds were also found in the ash, for example, quartz, albite and microklin in the boiler ash.

Despite the limitations of the analysis, one can conclude that no large changes occurred in the crystalline part of the ashes. The cyclone ash in all cases had a high NaCl content, but only the Ref case contained KCl. Regarding the fact that high concentrations of small NaCl crystals in the cyclone ash can impede good analytical results, the samples were washed with deionized water, dried, and then reanalyzed. However, the washing had only a small impact on the results in these cases. Calcium aluminum oxide, calcium aluminum silicate and quartz were the dominant compounds in all cases, and only one phosphate was detected in one case, that of AW.

3.6. Chemical Analysis of Ashes

Five ash fractions were analyzed (see Figure 10). The comparison indicates increasing concentrations of S, Cl, and Ca when following the system from bed ash—the first fraction sampled—to filter ash. However, for Al, Si, and alkali the reverse is the case, with the lowest concentrations being found in the filter ash. This could be explained by the smaller amount of sand particles, consisting mostly of Si, Al, K, and Na, in the filter ash.

Once more, higher concentrations of Ca, P, S, and Cl could be observed in the ashes in the AW case. For S and Cl, this is more noteworthy given that S and Cl concentrations in the fuel in both the Ref and AW cases were fairly similar (Figure 3). This may be linked to the lower bed temperature because the results are close to those from the RBT case, in which the lower bed temperature led to higher capture of S and Cl in the bed material coating [8]. Ca and P, mainly introduced as bone tissue

with the AW, seem to be enriched in the bed ashes. The results for K and Na in Table 3 reconfirm that no major differences of the alkali concentration could be seen between the two cases.

Table 2. XRD results from the Ref and AW cases.

Compound	Boiler ash		Cyclone ash		Filter ash		Fresh Sand
	Ref	AW	Ref	AW	Ref	AW	
$Ca(OH)_2$	L	L	-	-	M	M	-
CaClOH	-	-	-	-	M	M	-
$CaCO_3$	-	-	L	L	L	L	-
CaO	L	L	T	T	-	-	-
$CaSO_4$	M	M	L	L	L	L	-
$Ca_5(PO_4)3(OH,CI,F)$	-	-	-	M	-	-	-
$Na_4Ca(SO_4)_3$	-	-	-	-	-	-	-
$Ca_3Al_2O_6$	M	M	M	M	-	-	-
$Ca_2Al_2SiO_7$	M	M	M	M	-	-	-
$CaSiO_3$	-	-	-	-	-	-	-
NaCl	-	-	L	L	M	M	-
KCl	-	-	L		M	M	-
SiO_2	M	M	M	M	-	-	M
$NaAlSi_3O_8$	M	M	-	-	-	-	M
$KAlSi_3O_8$	L	M	-	-	-	-	M
$Na_2Si_2O_5$	-	-	-	-	-	-	-
Fe_2O_3	T	-	-	-	-	-	-
Al metall	-	-	L	L	-	-	-
Fe metall	L	-	-	-	-	-	-
MgO	M	M	-	-	-	-	-
$(Mg,Al)_6(Si,Al)_4O_{10}(OH)_8$ Clinochlore	-	-	-	-	-	-	M

Notes: M = Much; L = Little; T = Trece.

Figure 10. Elemental analysis of bed ash, return sand, boiler ash, cyclone ash, and filter ash, for the Ref and AW cases.

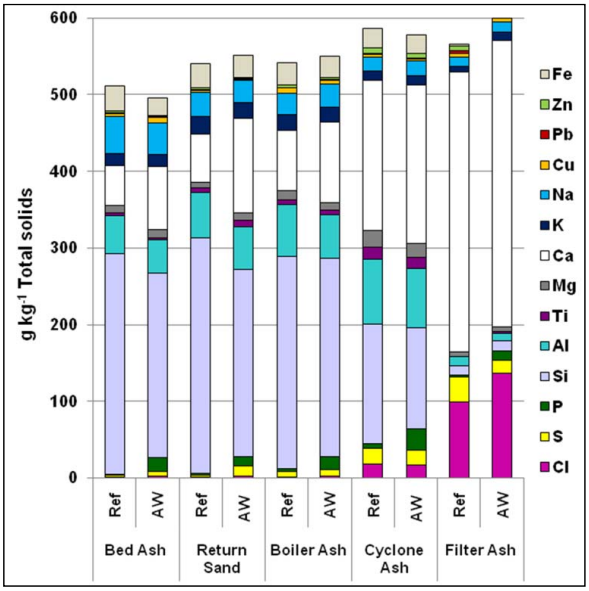

Table 3. Elemental analysis of ashes [g (kg ash)$^{-1}$].

Element	Bed Ash		Return Sand		Boiler Ash		Cyclone Ash		Filter Ash	
	Ref	AW	Ref	AW	Ref	AW	Ref	AW	Ref	AW
Cl	1.0	3.0	0.9	2.4	1.4	2.0	18	17	99	137
S	2.6	5.8	3.1	13	7.2	9.3	21	19	33	17
P	1.9	18	1.8	13	3.4	17	6.2	28	2.1	11
Si	287	241	307	244	277	258	156	132	13	14
Al	49	43	60	56	68	57	84	77	11	10
Ti	3.1	3.3	5.5	8.4	6.2	6.0	16	15	1.0	1.7
Mg	10	11	7.6	10	12	9.3	21	18	6.1	6.7
Ca	52	82	63	123	79	105	196	206	365	373
K	16	15	24	20	21	20	12	12	7.4	11
Na	48	42	31	30	28	30	19	19	12	14
Cu	4.6	7.0	3.0	1.4	6.6	5.3	4.1	3.5	5.3	4.8
Pb	0.7	0.4	0.7	0.3	0.6	0.4	0.9	0.7	3.5	2.4
Zn	2.5	1.9	3.0	2.1	3.8	2.5	7.0	5.8	5.2	3.3
Fe	33	23	31	29	29	28	26	24	3.4	2.3

Figure 11 presents the elemental balances over the boiler for the various fractions. The results were calculated using the measured ash and fuel flows, in addition to the chemical compositions of both fuels and ashes. The fractions entering the system are fuel and lime and the fractions coming out are the ash fractions. The element balances agree very well, considering the size of the boiler.

Figure 11. Element balances over the boiler: (**a**) Ref case; (**b**) AW case. X = The total inflow of the element to the boiler (fuel and lime) compared to the outflow (ash flows).

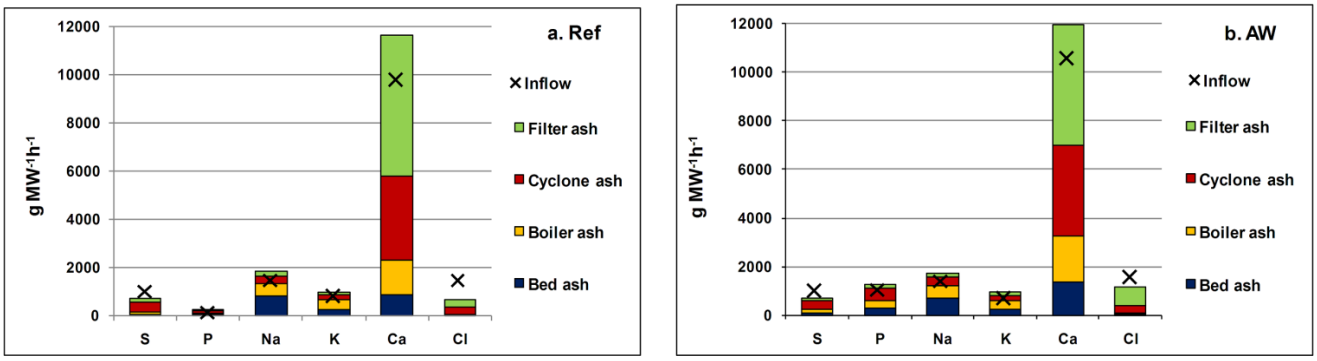

(**a**) (**b**)

Table 4 presents more detailed information about the proportion of elements in different ash fractions. As a result of AW co-combustion, the proportion of total P increased from 15% to 23% in the bed ash but decreased from 46% to 40% in the cyclone ash. The Ca concentration increased by 2.7 and 3.6 percentage points in the bed ash and boiler ash, respectively, but decreased by 6.6 percentage points in the filter ash. The S concentrations rose by approximately 8 percentage points in the bed ash and boiler ash, but declined by 1percentage points in the cyclone ash and 20 percentage points in the filter ash. The total alkali decreased by 13 percentage points in the bed ash, but increased in the boiler, cyclone and filter ashes. The greatest reduction in Cl concentration was observed in cyclone ash, in which it decreased by over 20 percentage points, while it increased by 1.5 percentage points in the bed ash.

Table 4. Elemental analysis balance of the ashes (wt-% distribution).

%Proportion in Ash	Bed Ash		Boiler Ash		Cyclone Ah		Filter Ash	
	Ref	AW	Ref	AW	Ref	AW	Ref	AW
P	13.6	23.3	25.7	24.8	46.8	40.0	13.9	12.0
Ca	7.5	11.4	12.1	15.9	30.2	31.2	50.2	41.6
S	4.1	11.4	12.1	20.0	34.6	41.6	49.2	27.0
K	27.9	25.8	38.2	36.3	21.8	23.0	12.2	14.8
Na	44.3	39.3	27.2	31.0	18.3	19.3	10.2	10.3
Cl	0.9	2.2	1.3	1.6	16.7	14.1	81.1	82.1

3.7. Bed and Agglomeration Temperature

Adding AW to the fuel mix, reduced the bed temperature by 70 °C relative to that of the Ref case. The positive effects of AW co-combustion on the bed agglomeration are shown in Figure 12a,b, in which visual inspection of the bed ashes for both cases shows considerably less amount of agglomerated particles in the AW case than do those from the Ref case. This difference could be explained by the change in temperature, the changed chemistry or both [8].

Figure 12. Bed ash samples: (**a**) Ref case, (**b**) AW case.

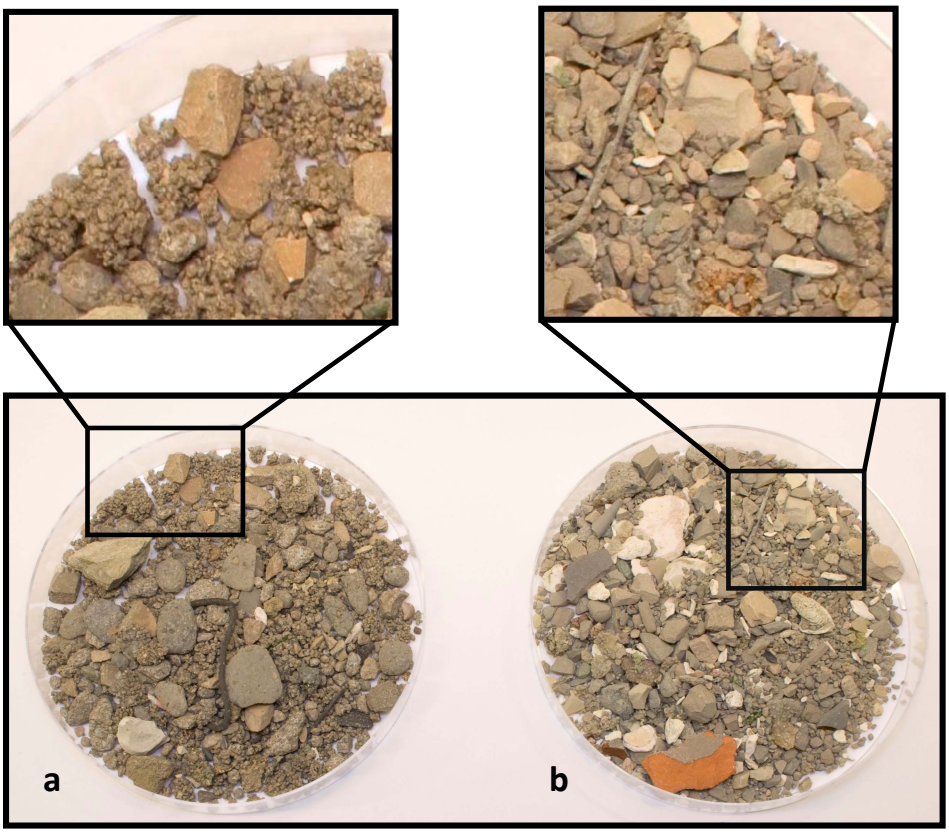

The results of the lab-scale bed agglomeration test are presented in Table 5. These results confirm that co-combustion of AW, with the normal waste fuel, increases the sintering temperature by 70–100 °C. However, the sintering temperatures in the tests are higher than the bed temperature in the full scale boiler.

Table 5. Agglomeration temperatures for return sand.

State	Unit	Ref	AW
Partial agglomeration	°C	953	981
Total agglomeration	°C	993	1079

3.8. Emission

Co-combustion of AW with MSW raises concern about higher NO_x emissions, regarding high concentration of nitrogen in the fuel. However, flue gas analysis indicated a reduction in NO_x emissions of approximately 50% when AW was added to the fuel mix, as seen in Figure 13. The NO_x-reduction effect of AW co-combustion has been reported previously [11]. The decrease in NO_x concentration in the flue gas, despite the much higher nitrogen content of the AW, could be explained by the release of nitrogen as ammonia (NH_3) during combustion. In the AW, nitrogen is found as amino acids, which are decomposed during thermal treatment, releasing the amino-group. However, the lower bed temperature and lower primary air flow are other possible explanations. Adding AW also resulted in a 50% lower demand for ammonia injection into the boiler, to reduce NO_x emission. In addition, SO_2 emissions also declined from 11 to under 1 mg per normal cubic meter of flue gas in the case of AW addition (Table 6). This might be due to a higher concentration of Ca and a lower concentration of S in the AW case fuel mix, leadings to the capture of S as $CaSO_4$ [24].

Figure 13. Emissions of N_2O, NO_x, and NH_3 together with ammonia addition to boiler No. 1 in the Ref and AW cases: (**a**) Ref; (**b**) AW.

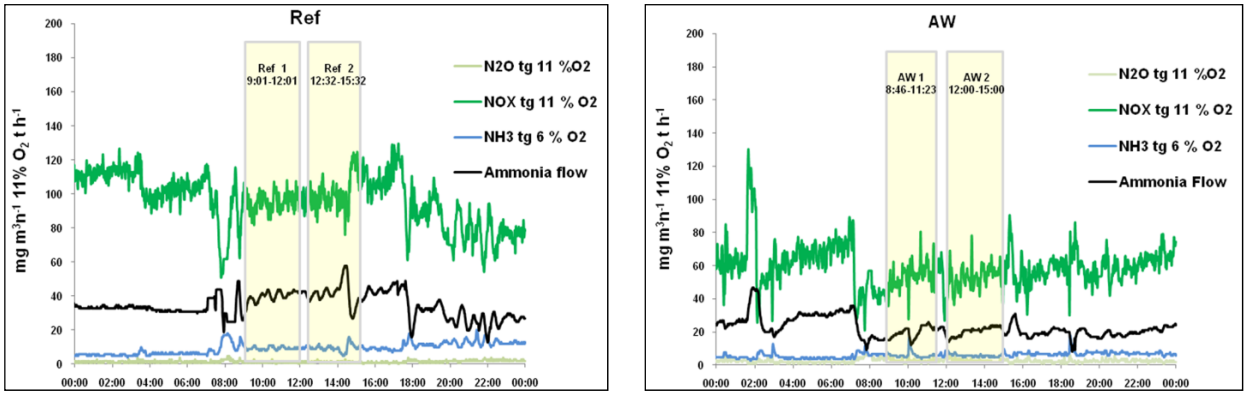

(**a**) (**b**)

Table 6. Flue gas emissions.

Compound	Unit	Ref	AW
NO_x	mg/Nm^3 11% O_2	95.5	53.0
N_2O	mg/Nm^3 11% O_2	1.4	3.0
NH_3	mg/Nm^3 11% O_2	6.3	4.2
SO_2	mg/Nm^3 11% O_2	11	0.5
HCl	mg/Nm^3 11% O_2	8.1	8.0

4. Conclusions

Adding 20–30 wt% AW to the ordinary waste fuel mix reduced the bed temperature by 70–100 °C and effectively reduced the deposition growth rate in the super heater area. Despite higher concentrations of Cl, alkali and S for the deposits formed in the AW case, there were no indications of higher corrosion. Inspection of the boiler after almost one year of operation also revealed no signs of increased corrosion damage.

SEM-EDX analysis of the coatings formed on return sand and bed ash particles indicated higher concentrations of P, Ca, S, and Cl in the bed material in the AW case; this was confirmed by the chemical fractionation analysis. In addition, chemical fractionation indicated that more acid-soluble compounds of P, Ca, and S were formed in the AW case. The increased amount of Ca and P, in the form of bone tissue, and P from the soft tissue introduced into the boiler by the AW did not affect the combustion, but appeared as calcium phosphates in the ashes. Positive effects of AW co-combustion were also observed in the bed, where agglomerates were found in the Ref case but not in the AW case.

The emission data indicated lower NO_x emissions in the AW case, despite a higher concentration of nitrogen in the AW fuel mix; this consequently reduced the rate of ammonia addition by 50%, relative to the Ref case. Later analyses indicated that the NO_x emissions from the boiler decreased to minimum levels and that ammonia addition could be completely stopped when adding 15–20 wt% of AW. Furthermore, SO_2 emissions declined during the co-combustion of AW, resulting in a decreased demand for added lime to capture sulfur.

Acknowledgments

This research was carried out under the auspices of Waste Refinery, an Excellence Centre for optimal conversion of waste, in Sweden. The full scale tests were performed by Borås Energy and Environment AB, Dalkia, the Technical Research Institute of Sweden (SP), and the University of Borås, which are all gratefully acknowledged. Furthermore, the authors acknowledge Metso Power AB and E.ON for their support during the project.

References

1. European Community. Directive 1999/31/EC of the European Parliament and of the Council of 26 April 1999 on the landfill of waste. *Off. J. Eur. Commun.* **1999**, *L182*, 1–17.
2. Karlfeldt, K.; Steenari, B.M. Assessment of metal mobility in MSW incineration ashes using water as the reagent. *Fuel* **2007**, *86*, 1983–1993.
3. Camerani Pinzani, M.C.; Somogyi, A.; Simionovici, A.S.; Ansell, S.; Steenari, B.-M.; Lindqvist, O. Direct determination of cadmium speciation in municipal solid waste fly ashes by synchrotron radiation induced μ-x-ray fluorescence and μ-x-ray absorption spectroscopy. *Environ. Sci. Technol.* **2002**, *36*, 3165–3169.
4. Miller, B.; Tillman, D. Fluidized-Bed Firing Systems. In *Combustion Engineering Issues for Solid Fuels*; Miller, B., Miller, S., Eds.; Elsevier: San Diego, CA, USA, 2008; pp. 277–340.

5. Skrifvars, B.J.; Westén-Karlsson, M.; Hupa, M.; Salmenoja, K. Corrosion of super-heater steel materials under alkali salt deposits. Part 2: SEM analyses of different steel materials. *Corros. Sci.* **2010**, *52*, 1011–1019.
6. Scala, F.; Chirone, R. An sem/edx study of bed agglomerates formed during fluidized bed combustion of three biomass fuels. *Biomass Bioenergy* **2008**, *32*, 252–266.
7. Karlfeldt Fedje, K.; Rauch, S.; Cho, P.; Steenari, B. Element associations in ash from waste combustion in fluidized bed. *Waste Manag.* **2010**, *30*, 1273–1279.
8. Pettersson, A.; Niklasson, F.; Moradian, F. Reduced bed temperature in a commercial waste to energy boiler—Impact on ash and deposit formation. *Fuel Process. Technol.* **2013**, *105*, 28–36.
9. Elled, A.-L.; Åmand, L.-E.; Leckner, B.; Andersson, B.-Å. The fate of trace elements in fluidised bed combustion of sewage sludge and wood. *Fuel* **2007**, *86*, 843–852.
10. Pettersson, A.; Åmand, L.-E.; Steenari, B.-M. Leaching of ashes from co-combustion of sewage sludge and wood—Part I: Recovery of phosphorus. *Biomass Bioenergy* **2008**, *32*, 224–235.
11. Herstad Svärd, S.; Backman, S.; Kullendorff, A.; Tilly, H.; Virta, L.; Sterngård, E. Co-Combustion of Animal Waste in Fluidized Bed Boilers-Operating Experiences and Emission Data. In Proceedings of the 17th International Conference on Fluidized Bed Combustion, Jacksonville, FL, USA, 18–21 May 2003; pp. 963–969.
12. Deydier, E.; Guilet, R.; Sarda, S.; Sharrock, P. Physical and chemical characterisation of crude meat and bone meal combustion residue: "Waste or raw material?". *J. Hazard. Mater.* **2005**, *121*, 141–148.
13. Jones, F.; Niklasson, F. Lowered Bed Temperature in a 20 MWth Waste Fired FB-Boiler- Effects on Ash Properties and Deposit Formation. In Proceedings of the 9th European Conference on Industrial Furnaces and Boilers, Estoril, Portugal, 26–29 April 2011.
14. Pettersson, A.; Zevenhoven, M.; Steenari, B.-M.; Åmand, L.-E. Application of chemical fractionation methods for characterisation of biofuels, waste derived fuels and CFB co-combustion fly ashes. *Fuel* **2008**, *87*, 3183–3193.
15. Pettersson, A.; Åmand, L.-E.; Steenari, B.-M. Chemical fractionation for the characterisation of fly ashes from co-combustion of biofuels using different methods for alkali reduction. *Fuel* **2009**, *88*, 1758–1772.
16. Teixeira, P.; Lopes, H.; Gulyurtlu, I.; Lapa, N. Use of chemical fractionation to understand partitioning of biomass ash constituents during co-firing in fluidized bed combustion. *Fuel* **2012**, *101*, 215–227.
17. Bendz, D.; Enell, A. *Metoder för Haltbestämning av Huvud- och Spårämnen och PAH i Jord och Avfall*; Report 13754; Swedish Geotechnical Institute and Swedish EPA: Linköping, Sweden, 2009.
18. Öhman, M.; Nordin, A. A new method for quantification of fluidized bed agglomeration tendencies: A sensitivity analysis. *Energy Fuels* **1998**, *12*, 90–94.
19. Brus, E.; Öhman, M.; Nordin, A.; Boström, D.; Hedman, H.; Eklund, A. Bed agglomeration characteristics of biomass fuels using blast-furnace slag as bed material. *Energy Fuels* **2004**, *18*, 1187–1193.
20. Öhman, M.; Nordin, A.; Skrifvars, B.-J.; Backman, R.; Hupa, M. Bed agglomeration characteristics during fluidized bed combustion of biomass fuels. *Energy Fuels* **2000**, *14*, 169–178.

21. Cascarosa, E.; Gea, G.; Arauzo, J. Thermochemical processing of meat and bone meal: A review. *Renew. Sustain. Energy Rev.* **2012**, *16*, 942–957.
22. Ebeledike, E.U.; Nwokedi, G.I.C.; Ndu, O.O.; Okoye, F.B.C.; Ochiogu, I.S. Calcium and phosphorus contents of body parts of some domestic animals used as meat source in nigeria. *Asian Pac. J. Trop. Med.* **2010**, *3*, 395–398.
23. Boström, D.; Grimm, A.; Boman, C.; Björnbom, E.; Öhman, M. Influence of kaolin and calcite additives on ash transformations in small-scale combustion of oat. *Energy Fuels* **2009**, *23*, 5184–5190.
24. Fryda, L.; Panopoulos, K.; Vourliotis, P.; Kakaras, E.; Pavlidou, E. Meat and bone meal as secondary fuel in fluidized bed combustion. *Proc. Combust. Inst.* **2007**, *31*, 2829–2837.